

Overexpression of ELF1 combined with MMP9 is associated with prognosis and tumor microenvironment in gastric cancer

XIAOXIA ZHANG^{1*}, XIAOYAN REN^{1*}, SHU ZHANG² and YAN WANG²

¹Department of Pathology, Affiliated Maternal & Child Care Hospital of Nantong University, Nantong, Jiangsu 226018, P.R. China;

²Department of Pathology, Affiliated Hospital of Nantong University, Nantong, Jiangsu 226001, P.R. China

Received April 11, 2024; Accepted July 26, 2024

DOI: 10.3892/etm.2024.12730

Abstract. Gastric cancer (GC) is a prevalent malignancy of the digestive system. E74-like factor 1 (ELF1) is a transcription factor that is specific to T cells and belongs to the Ets family. They are typically expressed in numerous tumor cells, such as pancreatic cancer, oral squamous cell, endometrial carcinoma, nasopharyngeal carcinoma and prostate and colorectal cancer, where they can promote cell invasion and migration. MMP9 is an important protease of the MMP family, since it serves a vital role in tumor progression and prognostic evaluation in colorectal cancer, uveal melanoma and clear cell renal cell carcinoma. The present study aimed to investigate the expression, correlation with MMP9 and clinical significance of ELF1 in GC. In addition, it aimed to explore the possible mechanisms. The ELF1 mRNA expression profile was first assessed using the GEPIA database and R4.2.1 software (Limma package). Reverse transcription-quantitative PCR (RT-qPCR) was used then to validate ELF1 mRNA expression levels in fresh GC samples from 40 patients. The clinical diagnostic value of ELF1 was also assessed using RT-qPCR. Tissue microarray immunohistochemistry (TMA-IHC) was utilized to examine the expression levels of ELF1 and MMP9 proteins in 355 paraffin-embedded GC samples. Subsequently, the present study further investigated the relationship between ELF1 and MMP9 and their possible effects on the clinicopathological features and prognosis of patients with GC. Gene correlation analysis was conducted using the GEPIA database and complemented with Tumor Immune Estimation Resource (TIMER) and CIBERSORT analyses to explore associations with immune infiltration. A significantly higher expression of ELF1 mRNA was found in GC tissues compared with

that in adjacent normal tissues ($P<0.05$). High ELF1 expression in GC tumor cells was found to distinguish GC tissues from adjacent normal tissues with a sensitivity of 87.5% and specificity of 77.5%. ELF1 and MMP9 proteins also showed higher expression in 355 GC compared with adjacent normal tissues, where they were significantly positively correlated ($P<0.001$). The two were closely associated with various clinicopathological features, including infiltration depth, lymph node involvement, metastasis, TNM staging, microscopic venous invasion, lymphatic invasion and blood serum carcinoembryonic antigen levels in GC. Furthermore, ELF1 and MMP9 expression levels were negatively associated with the overall survival of patients with GC. Prognostic analysis using the Cox proportional hazards model identified high ELF1 expression [hazards ratio (HR), 2.555; 95% CI, 1.546-4.224; $P=0.002$], high MMP9 expression (HR, 3.813; 95% CI, 2.406-6.041; $P<0.001$), advanced TNM stage ($P=0.001$) and advanced N stage ($P=0.011$) to be independent prognostic factors for patients with GC. Correlation analysis results from the GEPIA database indicated significant associations of ELF1 expression with various GC-related genes, including MutL homolog 1, erythroblastic leukemia viral oncogene homolog 2, PI3K catalytic subunit α , and tumor suppressor protein 53, MMP-9, Cadherin 1, TIMP1, growth factor A and kinase insert domain receptor. In addition, immune infiltration correlation analysis on TIMER and CIBERSORT revealed ELF1 positive relationship with specific infiltrating immune cell types, including naive B, memory-activated CD4⁺ and gamma delta T cells, and activated NK cells ($P<0.05$). This observation was further confirmed using immunohistochemistry, showing that ELF1 was associated with CD19 (B-cells) ($P<0.001$) and CD4 (CD4⁺ T cells, $P=0.002$). In conclusion, results from the present study suggest that ELF1 is overexpressed in GC. ELF1 combined with MMP9 can serve as a predictor of malignant biological behavior in GC and therefore a prognostic indicator for patients, due to its association with the tumor microenvironment.

Correspondence to: Dr Yan Wang, Department of Pathology, Affiliated Hospital of Nantong University, 20 Xisi Road, Nantong, Jiangsu 226001, P.R. China
E-mail: yisheng_wangyan@126.com

*Contributed equally

Key words: E74-like factor 1, MMP9, gastric cancer, prognosis, tumor microenvironment

Introduction

As a prevalent gastrointestinal malignancy, gastric cancer (GC) is distinguished by its high incidence, aggressive progression profile and high mortality rates. There were >968,000 novel cases of stomach cancer in 2022 and close to 660,000 deaths,

ranking the disease as fifth in terms of both incidence and mortality worldwide (1). Despite a decline in the global prevalence and death rate of GC, rates remain high in Eastern Asian countries (2). The majority of patients with GC are typically diagnosed already at advanced stages during consultations, resulting in a poor prognosis post-surgery. This scenario poses considerable public health challenges (3). Consequently, the quest for efficacious molecular markers for GC assumes paramount importance in facilitating precise treatment design, extending patient survival and enhancing their overall quality of life.

The primary approach for treating GC continues to involve conventional surgical procedures, followed by postoperative radiotherapy and chemotherapy (4). However, the 5-year survival rate following surgery remains low (<10%) (5). With the rapid advancement of molecular biology research, GC treatment methods have undergone continuous improvements, including the introduction of immunotherapy, such as programmed cell death protein (PD)-1/PD-L1 inhibitors and cytotoxic T lymphocyte antigen 4 inhibitors (6). Additionally, the emergence of chemotherapeutic and molecular-targeted drugs, such as oxaliplatin and herceptin, has instilled optimism among patients with intermediate and advanced stages of GC. Although these interventions have led to improved postoperative survival rates, the prognosis for GC, particularly in cases in, remains poor due to the severe toxic side effects, limited sensitivity and specificity of drugs (7). This is especially the case in patients at intermediate and advanced stages (7). The metastatic propensity of GC represents a formidable obstacle in the treatment paradigm (8).

Therefore, the exploration of effective strategies to inhibit GC's metastatic spread and identification of molecular markers for prognostic assessment is required.

E74-like factor 1 (ELF1), which is highly homologous to the *Drosophila* E74 factor (9) is a transcription factor inducible by ecdysone in *Drosophila* and a member of the Ets transcription factor family (9). ELF1 is located on chromosome 13q13 and consists of 619 amino acid residues, possessing the ability of both transcriptional activation and repression of target genes depending on the physiological context. Posttranslational processing determines its subcellular localization, biological activity and metabolic degradation (10). The functional regulation of ELF-1 is complex. ELF1 protein exists in a 80-kDa form in the cytoplasm and enters the nucleus in a 98 kDa form after phosphorylation and glycosylation (11). It is predominantly expressed in lymphocytes, where its posttranslational modifications bestow ELF1 with regulatory functions, enabling it to bind to gene promoters or enhancers critical for the selection, survival and maturation of diverse immune cells (12). The importance of ELF1 extends to its association with the development and metastasis of various malignancies (13), such as glioma, oral squamous cell carcinoma, endometrial carcinoma, nasopharyngeal carcinoma and prostate cancer, and colon cancer. Long non-coding RNAs (lncRNAs) are associated with cancer progression in GC (14). E2F transcription factor 1 has been shown to activate the transcription of terminal differentiation-induced non-coding RNA by binding to its promoter region, thereby promoting the proliferation of GC cells and inhibiting apoptosis (15). lncRNAs NONHSAT057282 and NONHSAG023333 can regulate genes associated with

chemoresistance, such as GSTP1, BTG3, SOCS3, and BRAC2, by interacting with the transcription factors ELF1 and E2F1. ELF1 may become a new player in chemoresistance through its interaction with different lncRNA interactions involved in tumor therapy (16). So, it was hypothesized that ELF1 may be associated with GC.

Tumor cells, together with extracellular matrix (ECM), cancer-associated fibroblasts (CAF), vascular-associated smooth muscle cells, pericytes, endothelial cells, mesenchymal stem and immune cells collectively constitute the complex tumor microenvironment (TME) (17). The development, progression and ultimately the prognosis of malignancies, are profoundly influenced by the characteristics of tumor cell invasion and metastasis (18). A pivotal process in this cascade involves ECM degradation, which is tightly regulated by MMPs and tissue inhibitors of metalloproteinases (TIMPs) (19). Among MMPs, MMP-9 is of particular importance as a key protease responsible for ECM degradation, where it serves a crucial role in various types of cancers, such as breast cancer (20,21). During cancer progression, ECM homeostasis is dynamically disrupted by MMP9, enabling cancer invasion and metastasis through the ECM barrier. MMP2 and MMP9 have been previously found to be upregulated in GC tissues (22). MMP9 rs3918242 polymorphism has been associated with the risk of various cancers, including lung, prostate, breast, and colorectal cancers (23). The chromosomal location (20q12-1q13) where MMP9 is located, has been identified as one of the most common regions of genomic gain in GC (24). Therefore, the progression of GC is highly likely to be influenced by altered MMP9 expression.

However, the precise expression pattern, interaction with MMP9 and predictive value of ELF1 in GC remain elusive. Therefore, the present study aimed to explore the expression profile of ELF1 in GC, its relationship with MMP9 and its (combined with MMP9) associations with various clinicopathological parameters, survival and prognosis of patients with GC. Bioinformatics and clinical sample analyses would be performed. In addition, relevant mechanisms, such as the association of ELF1 with epithelial-mesenchymal transition (EMT), angiogenesis and immune infiltration, were explored.

Materials and methods

Clinical patient samples. Fresh GC and adjacent normal tissues (located >2 cm from the tumor margin) were randomly collected from 40 patients post-GC surgery at the Affiliated Hospital of Nantong University (Nantong, China) from November to December 2021. This cohort included 28 males and 12 females, with a mean age of 66.25 years (range, 36-92 years; Table SI). The inclusion criteria were as follows: i) Pathological diagnosis of GC; ii) clinical data and overall survival time were complete; iii) no history of antitumor treatment before surgery and iv) no combination of other organic disease and malignant tumors. The exclusion criteria were as follows: i) incomplete clinical data and overall survival time; ii) combined with other organic diseases and malignant tumors; iii) a history of preoperative antitumor treatment; and iv) use of pathological case data without the patient's informed consent. Necrotic tissues were excised and blood contaminants were rinsed with saline before the samples were frozen at -80°C for further analysis.

Additionally, 355 paraffin-embedded GC specimens and corresponding adjacent normal tissues from the patients undergoing surgery from January 2013 to December 31, 2015, preserved in the Department of Pathology of Affiliated Hospital of Nantong University (Nantong, China, were collected from January 2019 to March 2019 for tissue microarrays for this study. The patients included 241 males and 114 females, with a mean age of 63.63 (range, 26-90) years. The inclusion and exclusion criteria were as aforementioned. The clinical characteristics collected included sex, age, histological type, differentiation, invasive depth (T), lymph node metastasis (N), distant metastasis (M), TNM stage, microvascular invasion (MVI), lymphatic invasion, perineural invasion, carcinoembryonic antigen (CEA), carbohydrate antigen 19-9 and Laurén classification (25). The cases that were processed and stained with H&E were pathologically confirmed on the basis of the latest WHO classification and 8th edition of the TNM classification recommended by the Union for International Cancer Control and American Joint Committee on Cancer (26). None of the patients had undergone any anticancer treatments, such as radiotherapy, chemotherapy or immunotherapy, before surgery. Complete clinical data and postoperative follow-up records (100% completion rate,) were obtained prior to the study. Overall survival (OS) was defined as the time from surgical resection to death or end of follow-up (December 31, 2020).

Reverse transcription-quantitative PCR (RT-qPCR) analysis for ELF1 mRNA expression in GC. The expression of ELF1 mRNA in the 40 fresh human GC tissue samples was validated through RT-qPCR. Total RNA was extracted from tissues by using a TRIzol kit (Invitrogen; Thermo Fisher Scientific, Inc.), which was then treated with DNase I (Cat No. D7073; Beyotime Institute of Biotechnology). The purity and concentration were analyzed using a NanoDrop ND-1000 spectrophotometer (Thermo Fisher Scientific, Inc.), followed by cDNA synthesis with a PowerScript™ Reverse Transcriptase kit (Bioland Scientific, LLC) according to the manufacturer's protocol. qPCR amplification was then performed on a 7500 real-time PCR system (Thermo Fisher Scientific, Inc.) using a SYBR® Premix ExTaq™ kit (Takara Bio, Inc.). The following thermocycling conditions were used: 95°C for 5 min for initial denaturation, followed by 40 cycles of 95°C for 10 sec (denaturation), 61°C for 20 sec (annealing) and 70°C for 40 sec (extension). The specific primers for ELF1 and the internal reference GAPDH were designed based on the NCBI gene sequence and synthesized by Shanghai Yingjun Biotechnology Co., Ltd. The specific forward primer for ELF1 was 5'-TGTCCAACAGAACGACCTAGT-3', whilst the reverse primer was 5'-GGCAGGAAAAATAGCTGGATCAC-3'. The length of the amplified target fragment was 88 bp. The forward primer of the GAPDH gene was 5'-GGA GCGAGATCCCTCCAAAAT-3', whereas the reverse primer was 5'-GGCTGTTGTCATACTTCTCATGG-3'. The length of the amplified target fragment was 197 bp. The results were analyzed by using the $2^{-\Delta\Delta C_q}$ method (27) with each sample assayed in triplicate.

Tissue microarray (TMA)-immunohistochemistry (IHC) for protein expression levels in GC. Postoperative GC and adjacent normal tissues from the 355 patients were fixed in

10% neutral formalin at room temperature for 24 h. Core tissue biopsy samples (0.2 cm in diameter) obtained from the paraffin-embedded blocks were arranged in fresh paraffin blocks using the Quick-Ray Manual Tissue Microarrayer Full Set (cat. no. UT06; Unitma, Co., Ltd.). In total, 12 tissue microarrays comprising 710 samples were ultimately prepared. Sections of 5- μ m thickness were analyzed for ELF1, MMP9, CD19, CD3, CD4, CD8 and CD56 protein expression levels by using immunohistochemistry. Sections were deparaffinized by immersion in xylene and rehydrated in gradient ethanol in separate batches, washed in PBS (0.01 M, pH=7.0), boiled (98°C, 20 min) under pressure in citrate buffer (0.01 M, pH=6.0; antigen recovered) and incubated with 5% goat-blocking serum (cat. no. SL039; Beijing Solarbio Science & Technology Co., Ltd.) in PBS for 30 min at 37°C to block non-specific binding. Subsequently, mouse antihuman ELF1 polyclonal antibody (dilution 1:400; cat. no. 22565-1-AP; ProteinTech Group, Inc.), MMP9 polyclonal antibody (dilution 1:300; cat. no. 10375-2-AP; ProteinTech Group, Inc.), mouse anti-human CD19 monoclonal (ready to use; cat. no. ZM-0038; ZSGB-BIO; OriGene Technologies, Inc.), mouse anti-human CD3 monoclonal (ready to use; cat. no. ZM-0417; ZSGB-BIO; OriGene Technologies, Inc.), mouse antihuman CD4 monoclonal (ready to use; cat. no. ZM-0418; ZSGB-BIO; OriGene Technologies, Inc.), rabbit anti-human CD8 monoclonal (ready to use; cat. no. ZM-0508 ZSGB-BIO; OriGene Technologies, Inc.) and mouse anti-human CD56 monoclonal (ready to use; cat. no. ZM-0057; ZSGB-BIO; OriGene Technologies, Inc.) were used for staining overnight at 4°C. HRP-labeled goat anti-mouse secondary antibody (1:1,000; cat. no. ab6728; Abcam) and HRP-labeled goat anti-rabbit IgG (1:1,000; cat. no. Ab6721; Abcam) were used at room temperature for 30 min. Sections were incubated with DAB (cat. no. DA1010; Beijing Solarbio Science & Technology Co., Ltd.) for ~10 min, counterstained with hematoxylin (room temperature, 20-30 sec) and sealed with gelatin glycerol. PBS served as a negative control. Staining results were double-blinded and analyzed by two senior pathologists (XYR and SZ).

Cells were light imaged through an optical microscope (BX51, OLYMPUS) of immunohistochemistry staining were defined as brownish-yellow or brownish-brown nuclei (ELF1) and cytoplasm (MMP9) staining of GC tumor cells, nuclei (ELF1) of the lymphocytes in mesenchyme, and membrane (CD19, CD3, CD4, CD8 and CD56) of infiltrated immune cells. The intensity was scored as follows: i) 0, negative; ii) 1, weak intensity; iii) 2, moderate intensity; and iv) 3, strong intensity. Percentage of positive cells was scored as follows: i) 0, negative; ii) 1, 1-25% positive; iii) 2, 26-50% positive; iv) 3, 51-75% positive; and v) 4, 76-100% positive. The multiplication of the two aforementioned scores was used as the final score, where 0-6 would be deemed no or low expression (-) and 7-12 was considered high expression (+) (28).

Bioinformatics analysis. Data on 375 primary GC tissues and 32 adjacent normal tissues were sourced from The Cancer Genome Atlas (TCGA) database (portal.gdc.cancer.gov/), where 'STAD' was searched to download RNA-Seq expression and clinical data for GC patients. Cases with gene expression of '0', lost-visit cases, and cases with incomplete clinical information were excluded by R language

(version 4.2.1). Gene Expression Profiling Interactive Analysis (GEPIA; <http://gepia.cancer-pku.cn/>) was used to compare ELF1 mRNA expression levels in GC and normal tissues. GEPIA is an interactive web server that can analyze RNA sequencing expression data from TCGA and GTEx for tumor and normal samples and can be used for numerous analyses, such as differential analysis, characterization based on cancer type or pathological stage, survival analysis, correlation analysis and downscaling analysis. The specific settings in 'Expression DIY' (Boxplot) were as follows: i) Gene symbol, ELF1; ii) Datasets Selection (Cancer name), stomach adenocarcinoma (STAD); iii) |Log₂fold change (FC)| Cutoff, 1; iv) P-value cut-off, 0.01; and v) Matched Normal data, Match TCGA normal and GTEx data. The Strawberry Perl software (version 5.38.2, perl.org/get.html) and R language (version 4.2.1) with Limma package (Log₂FC filter >1; adjusted P-value filter=0.05; Wilcox test) were used to obtain the ELF1 mRNA expression differentiation. Strawberry Perl software was used to convert probe names from transcriptome files to gene names, and 'Limma' was used for analyzing chip data.

GEPIA was also utilized for various correlation analyses, including the analysis of correlations between ELF1 and expressions of GC molecular typing-related genes, including MutL homolog 1 (MLH1), erythroblastic leukemia viral oncogene homolog 2 (ERBB2), PI3K subunit α (PIK3CA) and p53 (29). EMT-related molecules, including MMP9, Cadherin 1 (CDH1) and TIMP1; and angiogenic indices, including vascular endothelial growth factor A (VEGFA) and kinase insert domain receptor (KDR). 'Correlation Analysis' was chosen on the database. Then ELF1 was designated as 'Gene A' for the x-axis, whilst other genes to be studied served as 'Gene B' for the y-axis. 'Pearson' was selected as 'Correlation Coefficient'. STAD tumor was selected from 'TCGA Tumor' dialog box to 'Used Expression Datasets'.

Tumor Immune Estimation Resource 2.0 (TIMER) (<https://cistrome.shinyapps.io/timer/>), a web server for the comprehensive analysis of infiltrated immune cells, is a resource for the systematic analysis of immune infiltrates among the different cancer types. The abundance of six infiltrated immune cell types (B cells, CD4+ T cells, CD8+ T cells, neutrophils, macrophages and dendritic cells) can be estimated using the TIMER algorithm (30). Users can conveniently access tumor immunological, clinical and genomic features by inputting function-specific parameters. 'Gene' module was chosen to visualize the scatter plots visualizing the correlation between ELF1 expression and different levels of infiltration by immune cell types in GC. 'Spearman' was selected as the 'Correlation Coefficient'.

Cell-type Identification By Estimating Relative Subsets Of RNA Transcript (CIBERSORT; version 2023.1.2, cibersort.stanford.edu/), a software for the deconvolution of transcriptome expression matrices to estimate the composition and abundance of immune components in mixed cells on the basis of linear support vector regression principles, was further applied to study the correlation of 22 immune cell scores with ELF1 expression levels (31). CIBERSORT was used to analyze immune cell content of each sample, those with a CIBERSORT output of P<0.05 were considered accurate and enrolled for further construction of the immune landscape, otherwise, samples were eliminated. Subsequently the correlation of ELF1 with these immune cells was analyzed.

Statistical analysis. Epidata 3.1 software (epidata.dk; Epidata Association from Denmark, was utilized to manage clinical and laboratory data. SPSS 21.0 (IBM Corp.) and GraphPad 5.0 software (Dotmatics) were used for data analysis. Wilcoxon signed-rank non-parametric test was used to analyze the experimental data from RT-qPCR, as it was non-normally distributed. MedCalc software (version 18.2.1, MedCalc Software Ltd.) was used for receiver operating characteristic (ROC) curve analysis to estimate the diagnostic value of ELF1. Categorical variables in IHC were compared by the χ^2 or Fisher exact tests, as appropriate. Survival curves were plotted by using the Kaplan-Meier method and tested through the log-rank test. Cox regression provided the hazard ratio (HR) and 95% CI in all prognostic analyses. P<0.05 was considered to indicate a statistically significant difference, association or correlation.

Results

Expression level of ELF1 mRNA in GC tissues. Examination in GEPIA revealed increased ELF1 mRNA expression in GC compared with normal gastric tissue (P<0.05; Fig. 1A). This trend was supported by results reported by the R4.2.1 software based on data from TCGA database (Fig. 1B and C). RT-qPCR assay was next performed to measure ELF1 mRNA expression in GC tissues, with an amplification efficiency of 99.33%. ELF1 mRNA expression in GC tissues was found to be significantly higher compared with that in adjacent normal tissues (P<0.05; Fig. 1D). Increased ELF1 mRNA expression was also revealed to be a reliable indicator for distinguishing GC tissues from normal adjacent tissues, as evidenced by an area under the curve of 0.8078 and a 95% CI of 0.7015-0.9141. The sensitivity and specificity of this differentiation were 87.5 and 77.5%, respectively (P<0.05; Fig. 1E).

Expression levels of ELF1 and MMP9 proteins in GC tissues. TMA-IHC revealed that the incidence of ELF1 (mainly localized to the nucleus) and MMP9 (mainly localized to the cytoplasm) positivity were statistically significantly higher in GC tissues compared with that in adjacent normal tissues (both P<0.001; Fig. 2 and Table I). However, no significant difference in the incidence of positive ELF1 expression in lymphocytes in the mesenchyme of GC tissues and adjacent normal tissues could be found (Fig. 2; Table I).

Correlations of ELF1 and MMP9 protein expression levels, their associations and clinical characteristics in GC. TMA-IHC revealed a positive association between the incidence of ELF1 and MMP9 positivity in GC tissues (P<0.001; Table II). ELF1 and MMP9 protein expression levels were also found to associate with T (both P<0.001), N (both P<0.001), M (ELF1, P=0.047; MMP9, P=0.001), TNM staging (both P<0.001), MVI (ELF1, P=0.040; MMP9, P=0.008), lymphatic invasion (ELF1, P=0.015; MMP9, P=0.017) and blood serum CEA levels (ELF1, P=0.002; MMP9, P<0.001; Table III). However, ELF1 expression in lymphocytes in the GC mesenchyme was not associated found to be with any of the clinicopathological parameters of patients with GC (Table III).

Association of ELF1 and MMP9 expression with the prognosis of patients with GC. Kaplan-Meier survival analysis

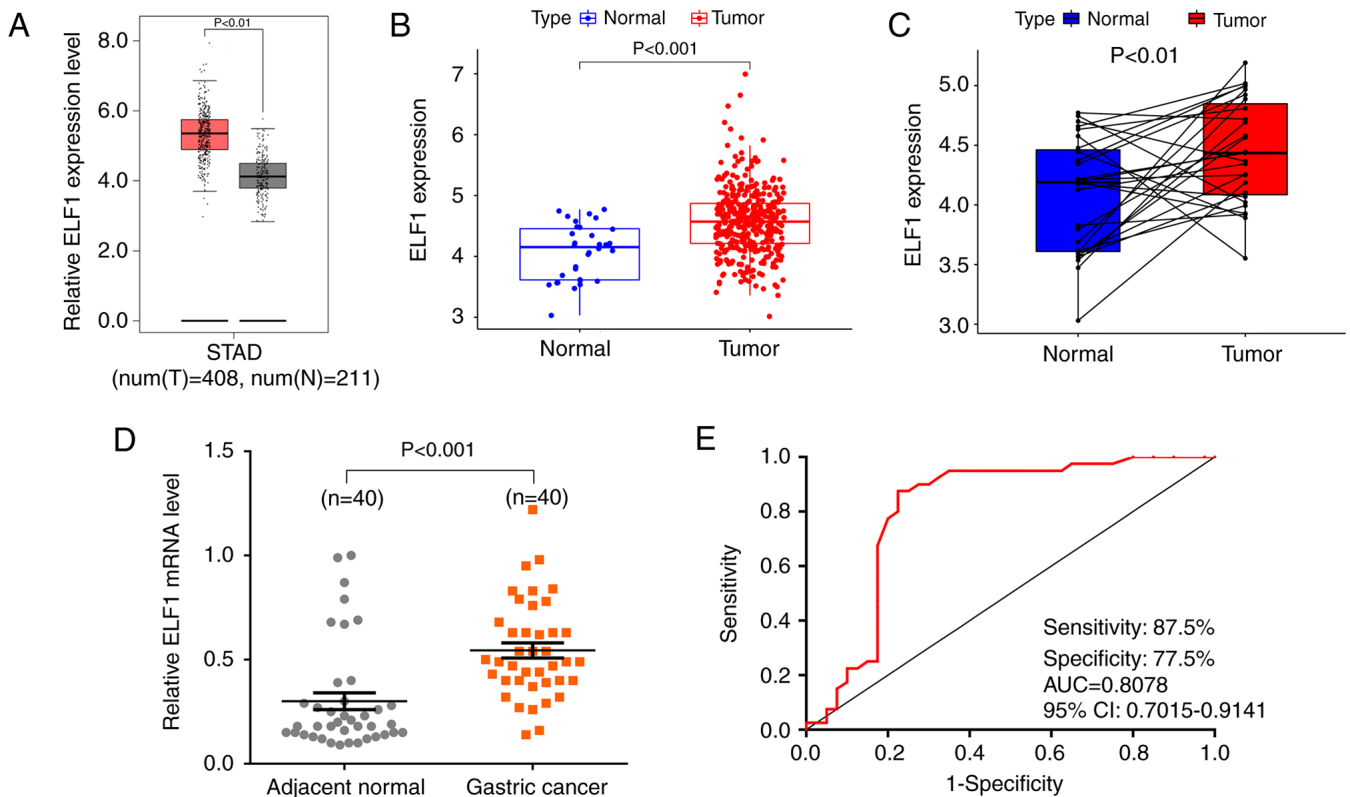


Figure 1. ELF1 mRNA expression and diagnostic value in GC tissues. (A) ELF1 mRNA expression levels in cancerous tissues (red) and adjacent normal tissues (black) obtained from the GEPIA database. (B) Boxplot of ELF1 mRNA expression in 375 GC tissues and 32 GC adjacent tissue samples in the TCGA database as investigated using the R software. (C) ELF1 mRNA expression in 375 GC tissues and 32 GC adjacent tissue samples in the TCGA database as investigated using the R software (linear diagram). (D) ELF1 expression in tissue from the 40 patients with GC was measured using reverse transcription-quantitative PCR. (E) Receiver operating characteristic curve. STAD, stomach adenocarcinoma; GC, gastric cancer; AUC, area under the curve; ELF1, E74-like Factor 1.

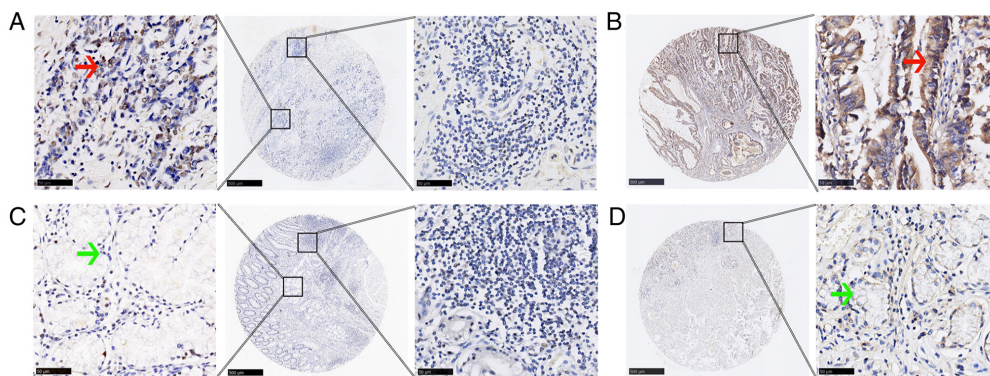


Figure 2. ELF1 and MMP9 protein expression levels in GC and adjacent normal tissues as detected by immunohistochemistry. (A) Left, positive ELF1 expression in GC tumor cells (red arrow); right, ELF1 expression in lymphocytes in the GC mesenchyme. (B) Positive MMP9 expression in GC tissues (red arrow). (C) Left, weakly positive ELF1 expression in adjacent normal epithelial cells (green arrow); right, ELF1 expression in lymphocytes in normal mesenchyme. (D) Weakly positive MMP9 expression in adjacent normal tissues (green arrow). Original magnification x400 (scale bars, 50 μ m); Smaller figures, original magnification x40 (scale bars, 500 μ m). ELF1, E74-like Factor 1; GC, gastric cancer.

revealed that patients with GC and elevated levels of ELF1 and MMP9 protein expression both faced significantly inferior overall survival (OS) compared with that in patients with lower expression levels of ELF1 and MMP9 proteins ($P<0.001$ for both; Fig. 3A and B). Specifically, OS stood at 17.1 and 11.5% in patients with high ELF1 and MMP9 expression levels, respectively. This is in contrast to that in patients with lower expression levels of ELF1 and MMP9 proteins, where the OS was observed to be 72.8% for ELF1 and 71.3% for

MMP9 (Fig. 3A and B). The lowest OS, which was 10.8%, was observed in patients with simultaneously high expression levels of ELF1 and MMP9 (Fig. 3C). In addition, OS decreased with increasing TNM stage ($P<0.001$; Fig. 3D). Further prognostic analysis using the Cox regression model showed that high ELF1 expression (HR, 2.555; 95% CI, 1.546-4.224; $P=0.002$), high MMP9 expression (HR, 3.813; 95% CI, 2.406-6.041; $P<0.001$), advanced TNM stage ($P=0.001$) and advanced N stage ($P=0.011$) were independent prognostic factors for

Table I. Expression of ELF1 and MMP9 by immunohistochemistry in GC and adjacent normal tissues (N=355).

Characteristic	Negative	Positive	P-value
GC	103 (29.0)	252 (71.0)	<0.001
Adjacent normal	245 (69.0)	110 (31.0)	
Characteristic	Negative	Positive	P-value
GC	129 (36.3)	226 (63.7)	<0.001
Adjacent normal	257 (72.4)	98 (27.6)	
Characteristic	Negative	Positive	P-value
GC	241 (67.9)	114 (32.1)	0.099
Adjacent normal	140 (62.0)	215 (38.0)	

ELF1, E74-like factor 1; GC, gastric cancer.

Table II. Association between ELF1 and MMP9 protein expression positivity in tissue microarray according to immunohistochemistry in patients with gastric cancer.

ELF1	MMP9		P-value
	-	+	
-	90	13	<0.001
+	39	213	

ELF1, E74-like factor 1.

patients with GC (Table IV). However, there was no significant association between ELF1 expression in lymphocytes in the GC mesenchyme and the prognosis of patients with GC (Table IV).

Gene correlation analysis. Investigations using the GEPIA database revealed notable positive associations between ELF1 expression and several crucial genes involved in GC occurrence (32). ELF1 expression showed a mild positive association with MLH1 ($r=0.35$; $P<0.001$), PIK3CA ($r=0.4$; $P<0.001$) and CDH1 ($r=0.39$; $P<0.001$; Fig. 4A-C), but not with ERBB2 ($r=0.16$), TP53 ($r=0.1$), MMP9 ($r=0.12$), TIMP1 ($r=-0.13$), VEGFA ($r=0.19$) and KDR ($r=0.16$; Fig. 4D-I). These findings suggest an association between ELF1 expression and the GC molecular subtypes, implying roles in various processes, such as EMT and angiogenesis.

Association between ELF1 expression and immune cell infiltration into GC. Infiltrating immune cell types into tumor tissues mainly include B-cells (CD19+), T-cells (CD3+, CD4+ and CD8+) and natural killer cells (NKs, CD56+) (33,34). The association between ELF1 expression and the infiltrating immune cells in GC was examined. TIMER database was used as an initial analysis to assess the correlation between the degree of infiltration by various immune cell types and ELF1 expression levels. This examination revealed no correlations between ELF1 expression and the levels of infiltration

by B cells ($r=0.187$), CD8+ T cells ($r=-0.017$), CD4+ T cells ($r=0.169$), Macrophage ($r=0.058$), neutrophil ($r=0.039$) or dendritic cells ($r=0.067$; Fig. 5A). Additionally, by using the CIBERSORT software, the relationship between ELF1 expression and infiltration by 24 subsets of different immune cell types integral to tumor immunity was evaluated. The outcomes revealed marked variations in several immune cell types across groups with differing ELF1 expression levels. In particular, ELF1 had a positive association with naive B cells ($P=0.028$), memory-activated CD4+ T cells ($P=0.009$), $\gamma\delta$ T cells ($P=0.029$) and activated NK cells ($P=0.001$), but no relationship with others. (Fig. 5B).

IHC was next used to further validate the relationship between ELF1 expression and infiltrating immune cells in GC. The results revealed that ELF1 had associations with CD19 (B-cells; $P<0.001$) and CD4 (CD4+ T cells; $P=0.002$), but not with CD3, CD8 or CD56 (Table V; Fig. 6).

Discussion

GC is a common malignant tumor worldwide and is characterized by high incidence and mortality rates, with multifactorial associations encompassing dietary habits (including high-fat intake, elevated salt consumption, and smoking), infections (such as *Helicobacter pylori* and Epstein-Barr virus infections) and genetic predispositions (35,36). Familial clustering is discernible in GC development, with ~25% of autosomal dominant diffuse GC-prone families harboring E-cadherin mutations (37). The aggressive and metastatic attributes of GC are closely associated with the poor patient prognosis, with a median survival of <12 months (38). Although significant improvements have been made in identifying biomarkers and molecular targeted agents (trastuzumab, Bevacizumab, Panitumumab, Everolimus, etc.) for improving patient prognosis, such as epidermal growth factor receptor (EGFR), vascular endothelial growth factor (VEGF) (39), mTOR and PI3K (40), predictive biomarkers and corresponding targeted agents specifically addressing GC invasion and metastasis remain scarce.

Ets genes, known for their erythroblast transformation specificity, constitute a class of highly conserved oncogenes that serve important roles in regulating tumor infiltration and metastasis (41). Among the genes in the Ets transcription factor family, ELF1 is one of the most prominent members (42). ELF1 is a T cell-specific transcription factor that was originally cloned from a human T-cell library through hybridization to a probe encoding the DNA-binding structural domain (Ets structural domain) of human Ets-1 cDNA. This transcription factor mainly exerts its influence by binding to gene promoters or enhancers (42) and can function to either activate and repress the expression of target genes. In addition, it is unique in being subject to glycosylation and phosphorylation (10). Elevated levels of ELF1 expression have been previously associated with the initiation and progression of various malignancies, such as pancreatic and colon cancer (13,43). The high expression of ELF1 has been associated with poor prognosis in patients with endometrial (44) and ovarian cancer (45). ELF1 can also promote the malignant progression of glioma (46). In addition, ELF1 has been found to promote the proliferation of oral squamous cell carcinoma cells by increasing the expression of β -catenin mRNA (47).

Table III. Association of ELF1 and MMP9 expression by tissue microarray-immunohistochemistry with clinical characteristics in patients with GC.

A, ELF1 expression				
Characteristic	N	Negative	Positive	P-value
Total	355	103 (29.0)	252 (71.0)	
Sex				0.204
Male	241	75 (31.1)	166 (68.9)	
Female	114	28 (24.6)	86 (75.4)	
Age				0.680
≤60	109	30 (27.5)	79 (72.5)	
>60	246	73 (29.7)	173 (70.3)	
Histological type				0.212
Tubular	246	71 (28.9)	175 (71.1)	
Papillary	7	2 (28.6)	5 (71.4)	
Mucinous	25	3 (12.0)	22 (88.0)	
Mixed (tubular and mucinous)	5	1 (20.0)	4 (80.0)	
Signet ring cell	72	26 (36.1)	46 (63.9)	
Differentiation				0.158
Well	55	14 (25.5)	41 (74.5)	
Middle	166	50 (30.1)	116 (69.9)	
Poor	104	35 (33.7)	69 (66.3)	
Others	30	4 (13.3)	26 (86.7)	
T				<0.001
Tis	6	5 (83.3)	1 (16.7)	
1	31	19 (61.3)	12 (38.7)	
2	60	23 (38.3)	37 (61.7)	
3	238	55 (23.1)	183 (76.9)	
4	20	1 (5.0)	19 (95.0)	
N				<0.001
0	145	58 (40.0)	87 (60.0)	
1	55	16 (29.1)	39 (70.9)	
2	84	19 (22.6)	65 (77.4)	
3	71	10 (14.1)	61 (85.9)	
M				0.047
0	339	102 (30.1)	237 (69.9)	
1	16	1 (6.3)	15 (93.8)	
TNM stage				<0.001
0+1	42	22 (52.4)	20 (47.6)	
2	115	52 (45.2)	63 (54.8)	
3	182	28 (15.4)	154 (84.6)	
4	16	1 (6.3)	15 (93.7)	
MVI				0.040
No	201	67 (33.3)	134 (66.7)	
Yes	154	36 (23.4)	118 (76.6)	
Lymphatic invasion				0.015
No	269	87 (32.3)	182 (67.7)	
Yes	86	16 (18.6)	70 (81.4)	
Perineural invasion				0.628
No	318	91 (28.6)	227 (71.4)	
Yes	37	12 (32.4)	25 (67.6)	

Table III. Continued.

A, ELF1 expression				
Characteristic	N	Negative	Positive	P-value
CEA (ng/ml)				0.002
≤5	122	48 (39.3)	74 (60.7)	
>5	219	52 (23.7)	167 (76.3)	
Unknown	14	3 (21.4)	11 (78.6)	
CA 19-9 (U/ml)				0.232
≤37	191	61 (31.9)	130 (68.1)	
>37	150	39 (26.0)	111 (74.0)	
Unknown	14	3 (21.4)	11 (78.6)	
Laurén classification				0.704
Intestinal type	260	74 (28.5)	186 (71.5)	
Diffuse type	95	29 (30.5)	66 (69.5)	
B, MMP9 expression				
Characteristic	N	Negative, N (%)	Positive, N (%)	P-value
Total	355	129 (36.3)	226 (63.7)	
Sex				0.418
Male	241	91 (37.8)	150 (62.2)	
Female	114	38 (33.3)	76 (66.7)	
Age				0.884
≤60	109	39 (35.8)	70 (64.2)	
>60	246	90 (36.6)	156 (63.4)	
Histological type				0.097
Tubular	246	85 (34.6)	161 (65.4)	
Papillary	7	4 (57.1)	3 (42.9)	
Mucinous	25	5 (20.0)	20 (80.0)	
Mixed (tubular and mucinous)	5	2 (40.0)	3 (60.0)	
Signet ring cell	72	33 (45.8)	39 (54.2)	
Differentiation				0.200
Well	55	20 (36.4)	35 (63.6)	
Middle	166	57 (34.3)	109 (65.7)	
Poor	104	45 (43.3)	59 (56.7)	
Others	30	7 (23.3)	23 (76.7)	
T				<0.001
Tis	6	5 (83.3)	1 (16.7)	
1	31	23 (74.2)	8 (25.8)	
2	60	33 (55.0)	27 (45.0)	
3	238	66 (27.7)	172 (72.3)	
4	20	2 (10.0)	18 (90.0)	
N				<0.001
0	145	73 (50.3)	72 (49.7)	
1	55	19 (34.5)	36 (65.5)	
2	84	22 (26.2)	62 (73.8)	
3	71	15 (21.1)	56 (78.9)	
M				0.001
0	339	129 (38.1)	210 (61.9)	
1	16	0 (0.0)	16 (100.0)	

Table III. Continued.

B, MMP9 expression				
Characteristic	N	Negative, N (%)	Positive, N (%)	P-value
TNM stage				<0.001
0+1	42	27 (64.3)	15 (35.7)	
2	115	61 (53.0)	54 (47.0)	
3	182	41 (22.5)	141 (77.5)	
4	16	0 (0.0)	16 (100.0)	
MVI				0.008
No	201	85 (42.3)	116 (57.7)	
Yes	154	44 (28.6)	110 (71.4)	
Lymphatic invasion				0.017
No	269	107 (39.8)	162 (60.2)	
Yes	86	22 (25.6)	64 (74.4)	
Perineural invasion				0.108
No	318	120 (37.7)	198 (62.3)	
Yes	37	9 (24.3)	28 (75.7)	
CEA (ng/ml)				<0.001
≤5	122	60 (49.2)	62 (50.8)	
>5	219	64 (29.2)	155 (70.8)	
Unknown	14	5 (35.7)	9 (64.3)	
CA 19-9 (U/ml)				0.017
≤37	191	80 (41.9)	111 (58.1)	
>37	150	44 (29.3)	106 (70.7)	
Unknown	14	5 (35.7)	9 (64.3)	
Laurén classification				0.386
Intestinal type	260	91 (35.0)	169 (65.0)	
Diffuse type	95	38 (40.0)	57 (60.0)	
C, ELF1 expression in lymphocytes				
Characteristic	N	Negative	Positive	P-value
Total	355	241 (67.9)	114 (32.1)	
Sex				0.525
Male	241	161 (66.8)	80 (33.2)	
Female	114	80 (70.2)	34 (29.8)	
Age				0.459
≤60	109	77 (70.6)	32 (29.4)	
>60	246	164 (66.7)	82 (33.3)	
Histological type				0.718
Tubular	246	165 (67.1)	81 (32.9)	
Papillary	7	5 (71.4)	2 (28.6)	
Mucinous	25	20 (80.0)	5 (20.0)	
Mixed (tubular and mucinous)	5	4 (80.0)	1 (20.0)	
Signet ring cell	72	47 (65.3)	25 (34.7)	
Differentiation				0.305
Well	55	40 (72.7)	15 (27.3)	
Middle	166	111 (66.9)	55 (33.1)	
Poor	104	66 (63.5)	38 (36.5)	
Others	30	24 (80.0)	6 (20.0)	

Table III. Continued.

C, ELF1 expression in lymphocytes				
Characteristic	N	Negative	Positive	P-value
T				0.988
Tis	6	4 (66.7)	2 (33.3)	
1	31	22 (71.0)	9 (29.0)	
2	60	40 (66.7)	20 (33.3)	
3	238	162 (68.1)	76 (31.9)	
4	20	13 (65.0)	7 (35.0)	
N				0.699
0	145	102 (70.3)	43 (29.7)	
1	55	34 (61.8)	21 (38.2)	
2	84	56 (66.7)	28 (33.3)	
3	71	49 (69.0)	22 (31.0)	
M				0.104
0	339	227 (67.0)	112 (33.0)	
1	16	14 (87.5)	2 (12.5)	
TNM stage				0.296
0+1	42	29 (69.0)	13 (31.0)	
2	115	80 (69.6)	35 (30.4)	
3	182	118 (64.8)	64 (35.2)	
4	16	14 (87.5)	2 (12.5)	
MVI				0.723
No	201	138 (68.7)	63 (31.3)	
Yes	154	103 (66.9)	51 (33.1)	
Lymphatic invasion				0.487
No	269	180 (66.9)	89 (33.1)	
Yes	86	61 (70.9)	25 (29.1)	
Perineural invasion				0.743
No	318	215 (67.6)	103 (32.4)	
Yes	37	26 (70.3)	11 (29.7)	
CEA (ng/ml)				0.756
≤5	122	81 (66.4)	41 (33.6)	
>5	219	149 (68.0)	70 (32.0)	
Unknown	14	11 (78.6)	3 (21.4)	
CA 19-9 (U/ml)				0.175
≤37	191	123 (64.4)	68 (35.6)	
>37	150	107 (71.3)	43 (28.7)	
Unknown	14	11 (78.6)	3 (21.4)	
Laurén classification				0.896
Intestinal type	260	176 (67.7)	84 (32.3)	
Diffuse type	95	65 (68.4)	30 (31.6)	

ELF1, E74-like factor 1; Tis, tumor in situ; MVI, microvascular invasion; CEA, carcinoembryonic antigen; CA19-9, carbohydrate antigen 19-9.

By contrast, ELF1 can activate the doublecortin-like kinase 1/Janus kinase/STAT signaling pathway, thereby promoting the malignant progression of pancreatic cancer (13). Another recent study has elucidated ELF1 effect on the biological behavior of colon cancer, which was by modulating the transcriptional

activation of serine peptidase inhibitor kazal type 4, thereby promoting colon cancer progression (43). However, conflicting reports exist that also suggest ELF1 to serve an inhibitory role in certain cancers, such as prostate cancer (48) and Hodgkin's lymphoma (49).

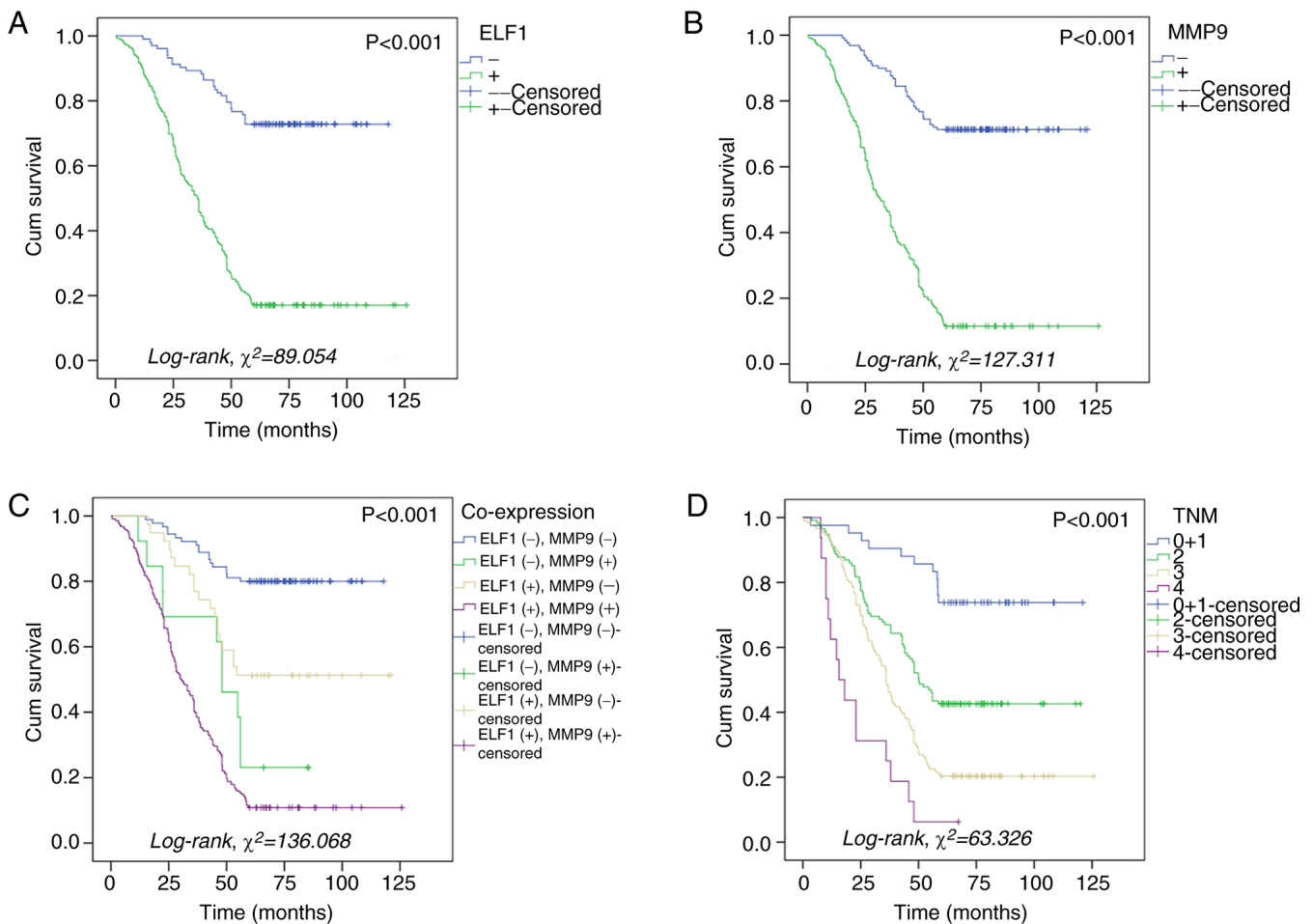


Figure 3. Kaplan-Meier survival analyses of patients with GC. (A) ELF1-high patients with GC (green line) exhibited inferior OS compared with those with ELF1-low expression (blue line). (B) MMP9-high patients with GC (green line) had inferior OS compared with that in MMP9-low patients (blue line). (C) Patients with GC and ELF1- and MMP9-high co-expression (purple line) had the worst OS among all groups compared. (D) Patients with the most advanced TNM stage had the shortest survival times. Censored data points indicate patients who were still alive until the end of follow-up. GC, gastric cancer; ELF1, E74-like Factor 1; Cum, cumulative; OS, overall survival.

The extracellular matrix (ECM) is divided into basement membrane and interstitial matrix, and is composed of various proteins such as type IV collagen, laminin, elastin, and hyaluronic acid, which provide structural support for cells and are also involved in the development of epithelial cells. The composition and stability of the ECM is closely related to the protein-protein and polysaccharide-protein binding in the extracellular matrix, which is one of the main barriers to prevent tumor metastasis. Degradation of ECM facilitates tumor cell invasion and metastasis and is a key trigger of EMT, where MMPs serve a key role because they can degrade almost all ECM components (50). The MMP family includes 26 different members, which can then be divided into various subtypes, including collagenases, gelatinases, matrix proteases and membrane-type MMPs (22). Previous studies have shown that MMP9 (a member of the gelatinase family), which can degrade the ECM and basement membranes, in addition to being associated with cancer cell adhesion and migration, is an important marker for predicting poor tumor prognosis in colorectal cancer (51) and endometrial carcinoma (44). In addition, MMP9 has been reported to positively correlate with the infiltration of a diverse range of immune cell types, including Th1 cells, neutrophils and macrophages, and

regulates their transport in uveal melanoma and clear Cell Renal Cell Carcinoma, which is essential for establishing and coordinating the tumor immune environment (52,53). The influence of MMP9 has been documented to extend to angiogenic and lymphangiogenic factors, such as VEGF, TGF- β , tumor necrosis factor- α , IL-8 and EGFR (54). Elevated levels of MMP9 mRNA and protein expression have been frequently found in various cancer types, including ovarian (55), colorectal (22), breast (56) and lung cancers (57). High MMP9 expression is also consistently associated with advanced tumor stages and adverse clinical outcomes, underscoring its potential as a prognostic indicator for patients with cancer of uveal melanoma and breast cancer (54,56).

Its family proteins enhance the expression of the urokinase-type plasminogen activator (uPA) gene by binding to its inducible enhancer region. uPA in turn activates a variety of MMPs (MMP1, MMP2 and MMP9) whilst promoting protein hydrolysis in the ECM (44). ELF1 serves a pivotal role in tumor angiogenesis, ECM remodeling and metastasis, by regulating various stages of neovascularization (which encompasses the generation of proangiogenic factors, MMPs and protease inhibitors) (58). In addition, ELF1 overexpression has been documented to contribute to a critical facet of tumor

Table IV. Cox regression analysis of prognostic factors for 5-year survival from gastric cancer.

Parameter	Univariate analysis		Multivariate analysis	
	HR (95% CI)	P-value	HR (95% CI)	P-value
ELF1 expression, high vs. low + none	5.519 (3.707-8.217)	<0.001	2.555 (1.546-4.224)	0.002
MMP9 expression, high vs. low + none	6.125 (4.291-8.744)	<0.001	3.813 (2.406-6.041)	<0.001
Age, ≤60 vs. >60 years	0.868 (0.662-1.138)	0.306		
Sex, male vs. female	0.978 (0.745-1.283)	0.870		
Histological type		0.043		0.803
Tubular vs. papillary	0.533 (0.170-1.669)	0.280	1.030 (0.315-3.365)	0.961
Tubular vs. mucinous	1.365 (0.849-2.194)	0.199	1.108 (0.672-1.828)	0.687
Tubular vs. mixed (tubular + mucinous)	2.023 (0.829-4.936)	0.121	0.900 (0.322-2.517)	0.841
Tubular vs. signet ring cells	0.716 (0.509-1.007)	0.055	0.811 (0.561-1.172)	0.266
Differentiation		0.064		
Well vs. middle	1.075 (0.744-1.553)	0.699		
Well vs. poor	0.828 (0.553-1.241)	0.361		
Well vs. others	1.557 (0.934-2.596)	0.090		
TNM stage		<0.001		0.001
0+1 vs. 2	2.992 (1.579-5.667)	0.001	4.440 (1.966-10.029)	<0.001
0+1 vs. 3	5.380 (2.908-9.956)	<0.001	4.983 (2.022-12.276)	<0.001
0+1 vs. 4	12.030 (5.494-26.345)	<0.001	8.796 (3.031-25.521)	<0.001
T trend		<0.001		0.179
Tis vs. 1	0.550 (0.146-2.072)	0.377	0.290 (0.070-1.197)	0.087
Tis vs. 2	1.406 (0.431-4.585)	0.572	0.365 (0.102-1.302)	0.120
Tis vs. 3	2.403 (0.767-7.525)	0.132	0.255 (0.069-0.935)	0.039
Tis vs. 4	3.243 (0.944-11.143)	0.062	0.219 (0.053-0.914)	0.037
N trend		<0.001		0.011
0 vs. 1	2.200 (1.512-3.201)	<0.001	1.452 (0.958-2.203)	0.079
0 vs. 2	2.750 (1.968-3.842)	<0.001	1.909 (1.275-2.859)	0.002
0 vs. 3	2.236 (1.562-3.200)	<0.001	1.273 (0.821-1.971)	0.280
M, 0 vs. 1	3.159 (1.866-5.348)	<0.001	0.919 (0.481-1.757)	0.799
MVI, no vs. yes	1.346 (1.043-1.737)	0.023	0.946 (0.718-1.246)	0.692
Lymphatic invasion, no vs. yes	1.275 (0.953-1.707)	0.102		
Perineural invasion, no vs. yes	1.316 (0.875-1.978)	0.187		
Carcinoembryonic antigen level, ≤5 vs. >5 ng/ml	1.645 (1.234-2.193)	0.001	0.690 (0.460-1.037)	0.074
Carbohydrate antigen 19-9 level, ≤37 vs. >37 U/ml	1.268 (0.977-1.646)	0.074		
Laurén classification, intestinal type vs. diffuse type	0.836 (0.622-1.125)	0.238		
ELF1 expression in lymphocytes, high vs. low and none	1.015 (0.772-1.334)	0.918		

HR, hazard ratio; ELF1, E74-like factor 1; Tis, Tumor in situ; MVI, microvascular invasion.

infiltration (pancreatic and colon cancer), namely ECM penetration. This was mediated through the transcriptional control of genes encoding enzymes involved in ECM degradation, such as MMP9 (59). The aforementioned findings suggest that ELF1 may regulate tumorigenesis and progression through the TME, which is associated with EMT, angiogenesis and immune infiltration. The present study revealed the expression profiles of ELF1 in GC, the possible mechanistic interplay between ELF1 and MMP9, in addition to their collective effect on patient survival and prognosis.

Initial analysis using the GEPIA database and R 4.2.1 software indicated elevated ELF1 expression in GC. Subsequently,

RT-qPCR analysis corroborated these findings, suggesting the diagnostic value of ELF1 expression in distinguishing GC from adjacent normal tissues. Therefore, it became possible to initially distinguish GC tissues from normal tissues based on ELF1 expression. Recent *in vitro* experiments showed that ELF1 overexpression directly activated MMP9 promoter activity, which identified an ELF1-triggered transcriptional mechanism by which neurotrauma upregulated MMP9 expression in the dorsal root ganglion (59). ELF1 has also been shown to activate forkhead box D3-antisense 1 to promote the migration, invasion and EMT of osteosarcoma cells by sponging microRNA-296-5p, preventing the inhibition of zinc

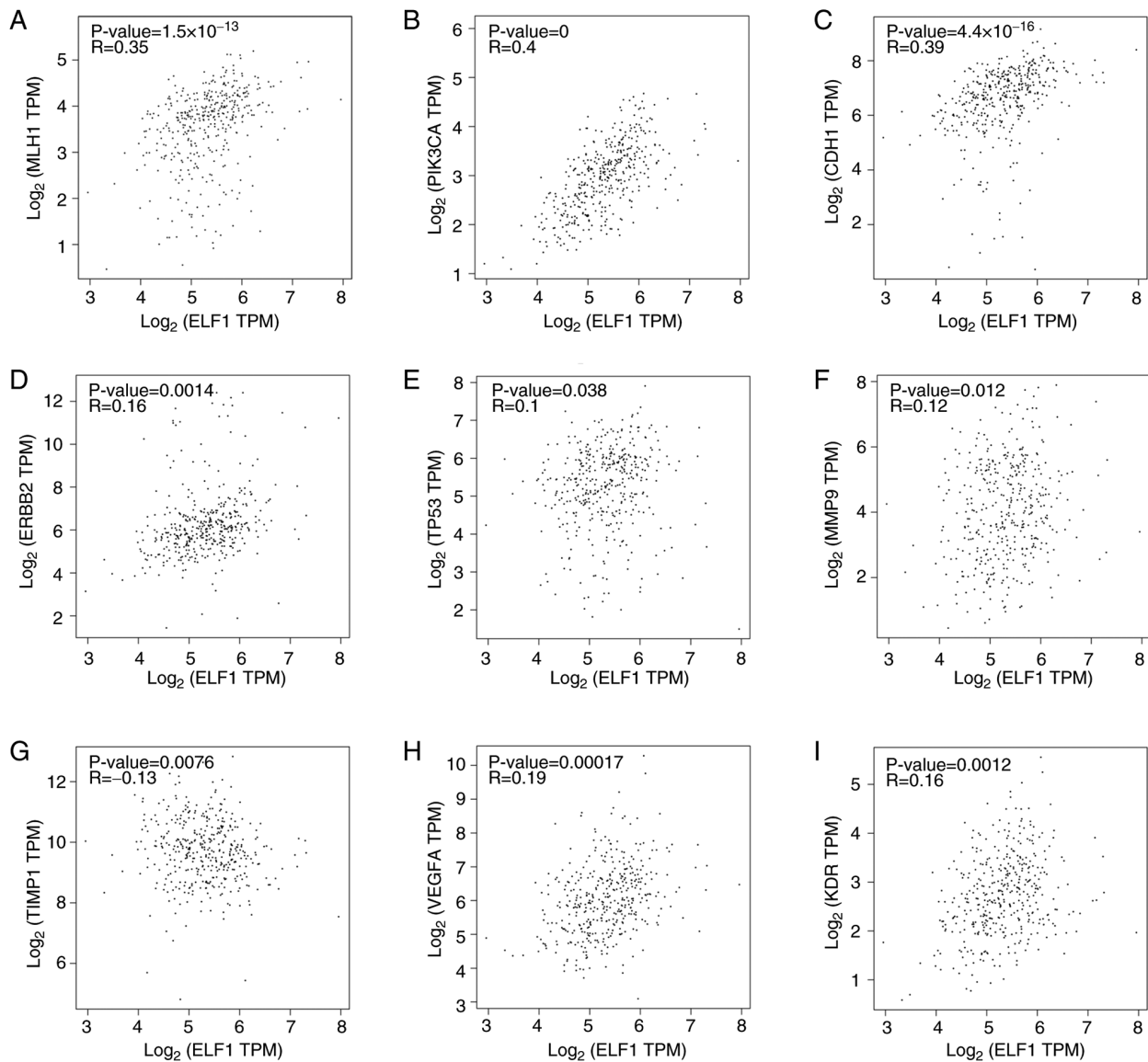


Figure 4. Correlation between ELF1 expression and that of MLH1, ERBB2, PIK3CA, TP53, MMP9, CDH1, TIMP1, VEGFA and KDR in GC tissues according to the GEPIA database. Correlation between ELF1 and (A) MLH1, (B) PIK3CA, (C) CDH1, (D) ERBB2, (E) TP53, (F) MMP9, (G) TIMP1, (H) VEGFA and (I) KDR. TPM, transcripts per kilobase of exon model per million mapped reads; ELF1, E74-like Factor 1; MLH1, MutL homolog 1; ERBB2, erythroblastic leukemia viral oncogene homolog 2; PIK3CA, PI3K subunit α ; CDH1, cadherin 1; TIMP1, tissue inhibitors of metalloproteinases; KDR, kinase insert domain receptor.

finger CCHC-type containing 3 (60). Transcription factor ELF1 activates MEIS1 transcription and promotes MEIS1 expression. Overexpression of MEIS1 increases growth factor independent protein 1) expression by activating the GF11 enhancer, but decreases FBW7 expression and thus promoting glioma cell proliferation (decreased PCNA), migration and invasive ability (decreased MMP-9), and reducing apoptosis (increased capase-3) promotes glioma development (46). ELF1 is involved in prostate cancer tumor cell migration and EMT by interfering with the oncogenic ETS function of ETS/Activator protein-1 cis-regulatory motifs (48). To elucidate the association between ELF1 and EMT in GC, TMA-IHC was performed. The results revealed increased levels of ELF1 and MMP9 proteins in GC tissues compared with adjacent normal tissues, where both exhibited positive associations with key clinical parameters, including T, N and M stages, TNM staging, MVI, lymphatic invasion and blood

CEA levels. Survival and prognostic analyses also revealed that patients with high expression levels of ELF1 and MMP9 proteins and advanced TNM staging had shorter survival and poorer prognoses. The findings of IHC revealed a positive correlation between the expression levels of ELF1 and MMP9. These findings suggest that high ELF1 expression may serve an important role in the pathogenesis and malignant progression of GC, which can be exploited to predict the survival and prognosis of patients with GC. However, the specific mechanistic interactions between ELF1 and MMP9 remain unclear, which require further study.

Based on heterogeneity of gastric cancer and the rapid development of molecular biology, TCGA proposed a molecular classification system for gastric cancer by analyzing data from multiple platforms, consisting of four distinct subtypes, including Epstein-Barr virus+ (accompanied by PIK3CA and ERBB2 amplification), microsatellite instability

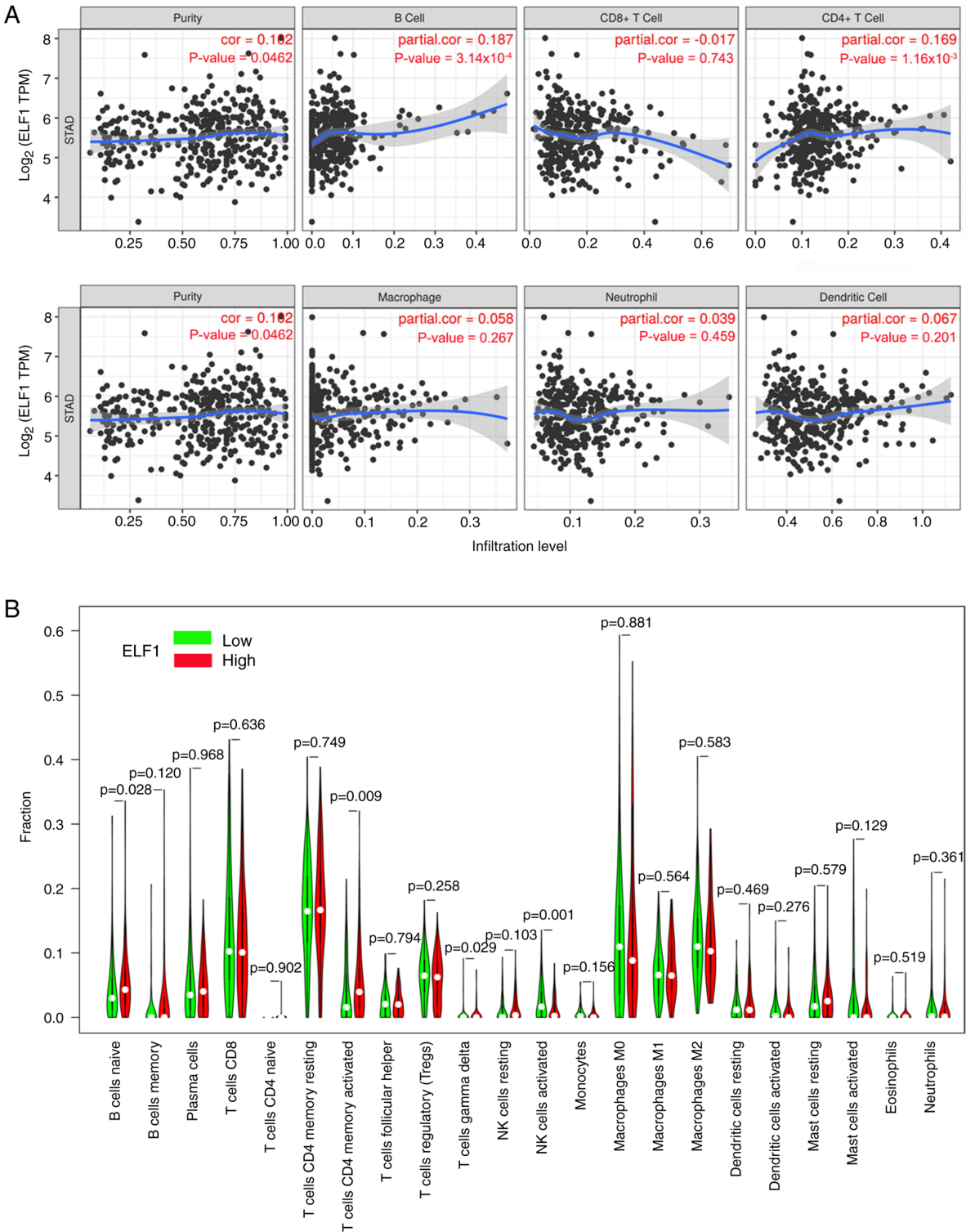


Figure 5. Connection between ELF1 expression and immune cell infiltration in GC. (A) Correlation analysis of ELF1 expression and the degree of infiltration by the various immune cell types according to TIMER. (B) Infiltration results between high and low expression groups of ELF1. ELF1, E74-like Factor 1; TPM, transcripts per kilobase of exon model per million mapped reads; NK, natural killer.

(usually accompanied by MLH1 silence, high-frequency mutation of ERBB2 and PIK3CA), genomically stable (accompanied by CDH1 gene mutation) and chromosome instability (accompanied by high mutation rates of TP53 and ERBB2 amplification (30). TIMP1, an endogenous inhibitor of MMP-9, executes a role not only in impeding the matrix degradation activity of MMP-9 whilst also activating pivotal

cytokines, including VEGF, TGF- α , TGF- β (transforming growth factor- β) and CAM (cell adhesion molecule), binding cell surface protein CD63, activating FAK-PI3K/AKT (focal adhesion kinase-phosphatidylinositol 3 kinase/protein kinase B) signaling pathway and MAPK) signaling pathway, leading to tumor cell proliferation (61). VEGFA and KDR are involved in tumor angiogenesis in addition to molecular

Table V. Association between ELF1 expression by tissue microarray-immunohistochemistry and that of different immune cell markers in GC.

ELF1	CD19		CD3		CD4		CD8		CD56	
	-	+	-	+	-	+	-	+	-	+
-	93	10	70	33	69	34	62	41	71	32
+	113	139	167	85	124	128	160	92	169	83
P-value	<0.001		0.759		0.002		0.560		0.733	

ELF1, E74-like factor 1.

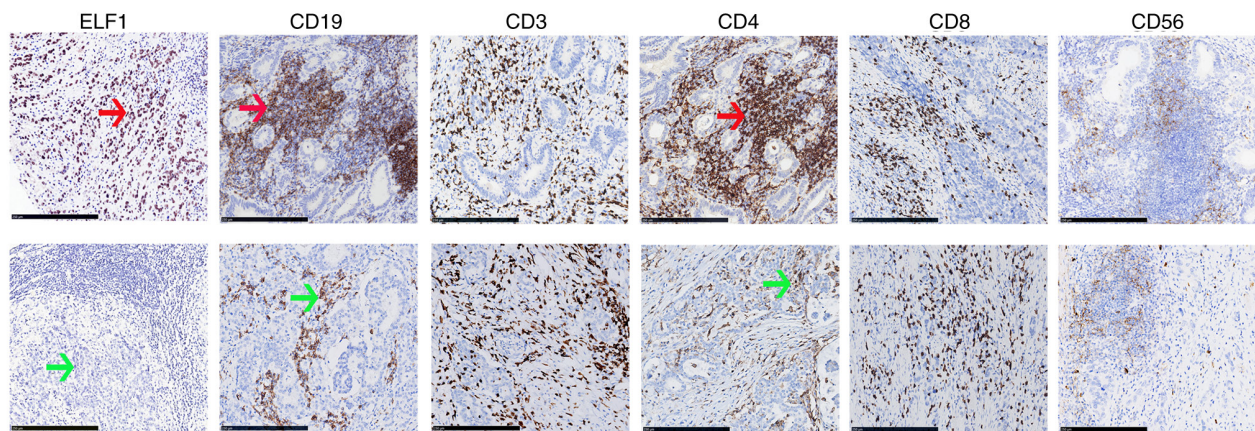


Figure 6. Association of ELF1 with CD19, CD3, CD4, CD8 and CD56 detected through immunohistochemical analysis. Magnification, x100; Scale bars, 250 μ m). The red arrow indicates area of high protein expression, whilst the green arrow indicates areas of low protein expression. Upper, GC with ELF1 (+); lower, GC with ELF1 (-). ELF1, E74-like Factor 1.

subtype identification of GC (62,63). The CDH1 gene encodes the vital cell adhesion molecule E-cadherin, which is crucial for maintaining epithelial tissue integrity. E-CAD reduction is associated with EMT, generation of stem-cell, and metastasis (64,65). Analysis of the GEPIA database in the present study revealed associations of ELF1 with MLH1, PIK3CA and CDH1. ELF1 has been previously reported to serve an indispensable role in the survival, differentiation and maturation of T and B lymphocyte cells, especially NK/T cells, where the absence of which results in T cell apoptosis (66). Findings from the TIMER database, CIBERSORT and IHC in the present study unveiled associations between ELF1 expression and B cells and CD4+ T cells. CD4+ and CD8+ T cells contribute to tumor growth and became effective targets for cancer survival, prognosis and treatment in lung cancer (67). B cells can produce cytokines (e.g., IL-10) that inhibit the antitumor response of T cells (inhibit CTL-mediated tumor clearance) and promote the production of immune complexes (generated by antitumor antibodies), inducing tumorigenesis. Breg (regulatory B) cells exhibit pro-tumorigenic activity due to a lack of response to CTLA4, resulting in a shortened overall survival in cutaneous melanoma, and produce adenosine, which is involved in the inhibition of T cell activation and/or inactivation influencing prognosis (such as urothelial bladder and gastric cancer) (68,69). CD4+ T cells can produce tumor cytokines (such as IL-4), associate with other cell types

(myeloid-derived suppressor cells and tumor-associated macrophages) and transform into regulatory T cells, which ultimately exert pro-tumorigenic functions (69,70). Based on the aforementioned results, we hypothesized that ELF1 appeared to be associated with GC development, which are intricately intertwined with the TME including EMT, angiogenesis and immune infiltration.

However, the present study has several limitations. All the specimens used for this study were selected randomly, and the size and quality of specimens could not be controlled. The detection of protein expression using IHC may be affected by tumor heterogeneity and subjective scoring system analysis. The selected tumor location may not accurately represent the entire tumor due to intratumor heterogeneity. In addition, the r-value of the correlation analysis based on data from the GEPIA database was low, which require confirmation through further detailed exploration in subsequent studies. The majority of the studies on the involvement of ELF1 in EMT and angiogenesis in GC were based on bioinformatics, where the exact mechanism and related signaling pathways requires further experimental verification. However, the results may provide guidance for future prospective clinical trials. Any future studies should conduct comprehensive and in-depth studies at the cytological and molecular levels to provide a solid theoretical foundation for the study of GC molecular targets.

Acknowledgements

Not applicable.

Funding

The present study was supported by the Nantong Science and Technology Program (grant no. JCZ19093).

Availability of data and materials

The data generated in the present study may be requested from the corresponding author.

Authors' contributions

YW designed the study. Data analysis was performed by XZ and XR. XZ drafted the article. XZ performed the experiments. Critical revision of article was done by SZ and YW. All authors approved the final version of the article. YW and XZ confirm the authenticity of all the raw data.

Ethics approval and consent to participate

The present study complies with the ethical standards of the Declaration of Helsinki (as revised in 2013) and was approved by the Ethics Committee of Affiliated Hospital of Nantong University (approval no. 2018-L042). Written informed consent was obtained by each patient or his or her family prior to this study.

Patient consent for publication

Not applicable.

Competing interests

The authors declare that they have no competing interests.

References

- Bray F, Laversanne M, Sung H, Ferlay J, Siegel RL, Soerjomataram I and Jemal A: Global cancer statistics 2022: GLOBOCAN estimates of incidence and mortality worldwide for 36 cancers in 185 countries. *CA Cancer J Clin* 74: 229-263, 2024.
- Lei ZN, Teng QX, Tian Q, Chen W, Xie Y, Wu K, Zeng Q, Zeng L, Pan Y, Chen ZS and He Y: Signaling pathways and therapeutic interventions in gastric cancer. *Signal Transduct Target Ther* 7: 358, 2022.
- Yeoh KG and Tan P: Mapping the genomic diaspora of gastric cancer. *Nat Rev Cancer* 22: 71-84, 2022.
- Sexton RE, Al Hallak MN, Diab M and Azmi AS: Gastric cancer: A comprehensive review of current and future treatment strategies. *Cancer Metastasis Rev* 39: 1179-1203, 2020.
- Sung H, Ferlay J, Siegel RL, Laversanne M, Soerjomataram I, Jemal A and Bray F: Global cancer statistics 2020: GLOBOCAN estimates of incidence and mortality worldwide for 36 cancers in 185 countries. *CA Cancer J Clin* 71: 209-249, 2021.
- Cai H, Li M, Deng R, Wang M and Shi Y: Advances in molecular biomarkers research and clinical application progress for gastric cancer immunotherapy. *Biomark Res* 10: 67, 2022.
- Zang YS, Dai C, Xu X, Cai X, Wang G, Wei J, Wu A, Sun W, Jiao S and Xu Q: Comprehensive analysis of potential immunotherapy genomic biomarkers in 1000 Chinese patients with cancer. *Cancer Med* 8: 4699-4708, 2019.
- Ajani JA, D'Amico TA, Bentrem DJ, Chao J, Cooke D, Corvera C, Das P, Enzinger PC, Enzler T, Fanta P, *et al*: Gastric cancer, version 2.2022, NCCN clinical practice guidelines in oncology. *J Natl Compr Canc Netw* 20: 167-192, 2022.
- Thompson CB, Wang CY, Ho IC, Bohjanen PR, Petryniak B, June CH, Miesfeldt S, Zhang L, Nabel GJ, Karpinski B, *et al*: cis-acting sequences required for inducible interleukin-2 enhancer function bind a novel Ets-related protein, Elf-1. *Mol Cell Biol* 12: 1043-1053, 1992.
- Tsokos GC, Nambiar MP and Juang YT: Activation of the Ets transcription factor Elf-1 requires phosphorylation and glycosylation: Defective expression of activated Elf-1 is involved in the decreased TCR zeta chain gene expression in patients with systemic lupus erythematosus. *Ann NY Acad Sci* 987: 240-245, 2003.
- Andrews PGP, Kennedy MW, Popadiuk CM and Kao KR: Oncogenic activation of the human Pygopus2 promoter by E74-like factor-1. *Mol Cancer Res* 6: 259-266, 2008.
- Hu M, Li H, Xie H, Fan M, Wang J, Zhang N, Ma J and Che S: ELF1 transcription factor enhances the progression of glioma via ATF5 promoter. *ACS Chem Neurosci* 12: 1252-1261, 2021.
- Yang B, Shen F, Zhu Y, Lu W and Cai H: E74-like ETS transcription factor 1 promotes the progression of pancreatic cancer by regulating doublecortin-like kinase 1/Janus kinase/signal transducer and activator of transcription pathway. *Am J Cancer Res* 14: 616-629, 2024.
- Zhang J, Chen L, Wei W and Mao F: Long non-coding RNA signature for predicting gastric cancer survival based on genomic instability. *Aging (Albany NY)* 15: 15114-15133, 2023.
- Xu TP, Wang YF, Xiong WL, Ma P, Wang WY, Chen WM, Huang MD, Xia R, Wang R, Zhang EB, *et al*: E2F1 induces TINCER transcriptional activity and accelerates gastric cancer progression via activation of TINCER/STAU1/CDKN2B signaling axis. *Cell Death Dis* 8: e2837, 2017.
- He DX, Zhang GY, Gu XT, Mao AQ, Lu CX, Jin J, Liu DQ and Ma X: Genome-wide profiling of long non-coding RNA expression patterns in anthracycline-resistant breast cancer cells. *Int J Oncol* 49: 1695-1703, 2016.
- Zeltz C, Primac I, Erusappan P, Alam J, Noel A and Gullberg D: Cancer-associated fibroblasts in desmoplastic tumors: Emerging role of integrins. *Semin Cancer Biol* 62: 166-181, 2020.
- Harrison JD and Fielding JW: Prognostic factors for gastric cancer influencing clinical practice. *World J Surg* 19: 496-500, 1995.
- Grzesiak M, Kaminska K, Knapczyk-Stwora K and Hrabia A: The expression and localization of selected matrix metalloproteinases (MMP-2, -7 and -9) and their tissue inhibitors (TIMP-2 and -3) in follicular cysts of sows. *Theriogenology* 185: 109-120, 2022.
- Wang Y, Chuang CY, Hawkins CL and Davies MJ: Activation and inhibition of human matrix metalloproteinase-9 (MMP9) by HOCl, myeloperoxidase and chloramines. *Antioxidants (Basel)* 11: 1616, 2022.
- Farina AR and Mackay AR: Gelatinase B/MMP-9 in tumour pathogenesis and progression. *Cancers (Basel)* 6: 240-296, 2014.
- Buttacavoli M, Di Cara G, Roz E, Pucci-Minafra I, Feo S and Cancemi P: Integrated multi-omics investigations of metalloproteinases in colon cancer: Focus on MMP2 and MMP9. *Int J Mol Sci* 22: 12389, 2021.
- Teng Z, Wang S, Yuan H, Wang H, Li J, Chang X, Zhang Y, Han Z and Wang Y: MMP-9 gene polymorphisms on cancer risk: An updated systematic review and meta-analysis. *Nucleosides Nucleotides Nucleic Acids* 3: 1-24, 2024.
- Fu CK, Chang WS, Tsai CW, Wang YC, Yang MD, Hsu HS, Chao CY, Yu CC, Chen JC, Pei JS and Bau DT: The association of MMP9 promoter Rs3918242 genotype with gastric cancer. *Anticancer Res* 41: 3309-3315, 2021.
- Costache S, Sajin M, Wedden S and D'Arrigo C: A consolidated working classification of gastric cancer for histopathologists (review). *Biomed Rep* 19: 58, 2023.
- Liu JY, Peng CW, Yang XJ, Huang CQ and Li Y: The prognosis role of AJCC/UICC 8th edition staging system in gastric cancer, a retrospective analysis. *Am J Transl Res* 10: 292-303, 2018.
- Livak KJ and Schmittgen TD: Analysis of relative gene expression data using real-time quantitative PCR and the 2(-Delta Delta C(T)) method. *Methods* 25: 402-408, 2001.
- Liao Q and Xiong J: YTHDF1 regulates immune cell infiltration in gastric cancer via interaction with p53. *Exp Ther Med* 27: 255, 2024.

29. Cancer Genome Atlas Research Network: Comprehensive molecular characterization of gastric adenocarcinoma. *Nature* 513: 202-209, 2014.
30. Li T, Fu J, Zeng Z, Cohen D, Li J, Chen Q, Li B and Liu XS: TIMER2.0 for analysis of tumor-infiltrating immune cells. *Nucleic Acids Res* 48 (W1): W509-W514, 2020.
31. Newman AM, Liu CL, Green MR, Gentles AJ, Feng W, Xu Y, Hoang CD, Diehn M and Alizadeh AA: Robust enumeration of cell subsets from tissue expression profiles. *Nat Methods* 12: 453-457, 2015.
32. Usui G, Matsusaka K, Mano Y, Urabe M, Funata S, Fukayama M, Ushiku T and Kaneda A: DNA methylation and genetic aberrations in gastric cancer. *Digestion* 102: 25-32, 2021.
33. Quan Q, Guo L, Huang L, Liu Z, Guo T, Shen Y, Ding S, Liu C and Cao L: Expression and clinical significance of PD-L1 and infiltrated immune cells in the gastric adenocarcinoma microenvironment. *Medicine (Baltimore)* 102: e36323, 2023.
34. Liu D, Heijl LR, Czigany Z, Dahl E, Lang SA, Ulmer TF, Luedde T, Neumann UP and Bednarsch J: The role of tumor-infiltrating lymphocytes in cholangiocarcinoma. *J Exp Clin Cancer Res* 41: 127, 2022.
35. Alhalabi MM, Alsaid SA and Albattah ME: Advanced diffuse gastric adenocarcinoma in young Syrian woman. A case report. *Ann Med Surg (Lond)* 78: 103728, 2022.
36. Tueli VC, Maiyoh GK and Ndombera FT: The role of infections in the causation of cancer in Kenya. *Cancer Causes Control* 33: 1391-1400, 2022.
37. Chang ZW, Dong L, Qin YR, Song M, Guo HY and Zhu QL: Correlations between gastric cancer family history and ROBO2 and RASSF2A gene methylations. *J Cancer Res Ther* 12: 597-600, 2016.
38. Tan AC, Chan DL, Faisal W and Pavlakis N: New drug developments in metastatic gastric cancer. *Therap Adv Gastroenterol* 11: 1756284818808072, 2018.
39. Li Z, Zhao Z, Wang C, Wang D, Mao H, Liu F, Yang Y, Tao F and Lu Z: Association between DCE-MRI perfusion histogram parameters and EGFR and VEGF expressions in different Lauren classifications of advanced gastric cancer. *Pathol Oncol Res* 27: 1610001, 2021.
40. He Y and Wang X: Identification of molecular features correlating with tumor immunity in gastric cancer by multi-omics data analysis. *Ann Transl Med* 8: 1050, 2020.
41. Hsing M, Wang Y, Rennie PS, Cox ME and Cherkasov A: ETS transcription factors as emerging drug targets in cancer. *Med Res Rev* 40: 413-430, 2020.
42. Oettgen P, Akbarali Y, Boltax J, Best J, Kunsch C and Libermann TA: Characterization of NERF, a novel transcription factor related to the Ets factor ELF-1. *Mol Cell Biol* 16: 5091-5106, 1996.
43. Li T, Jia Z, Liu J, Xu X, Wang H, Li D and Qiu Z: Transcription activation of SPINK4 by ELF-1 augments progression of colon cancer by regulating biological behaviors. *Tissue Cell* 84: 102190, 2023.
44. Takai N, Miyazaki T, Nishida M, Shang S, Nasu K and Miyakawa I: Clinical relevance of Elf-1 overexpression in endometrial carcinoma. *Gynecol Oncol* 89: 408-413, 2003.
45. Takai N, Miyazaki T, Nishida M, Nasu K and Miyakawa I: The significance of Elf-1 expression in epithelial ovarian carcinoma. *Int J Mol Med* 12: 349-354, 2003.
46. Cheng M, Zeng Y, Zhang T, Xu M, Li Z and Wu Y: Transcription factor ELF1 activates MEIS1 transcription and then regulates the GF11/FBW7 axis to promote the development of glioma. *Mol Ther Nucleic Acids* 23: 418-430, 2020.
47. Qiao C, Qiao T, Yang S, Liu L and Zheng M: SNHG17/miR-384/ELF1 axis promotes cell growth by transcriptional regulation of CTNNB1 to activate Wnt/ β -catenin pathway in oral squamous cell carcinoma. *Cancer Gene Ther* 29: 122-132, 2022.
48. Budka JA, Ferris MW, Capone MJ and Hollenhorst PC: Common ELF1 deletion in prostate cancer bolsters oncogenic ETS function, inhibits senescence and promotes docetaxel resistance. *Genes Cancer* 9: 198-214, 2018.
49. Paczkowska J, Soloch N, Bodnar M, Kiwerska K, Janiszewska J, Vogt J, Domanowska E, Martin-Subero JI, Ammerpohl O, Klapper W, *et al*: Expression of ELF1, a lymphoid ETS domain-containing transcription factor, is recurrently lost in classical Hodgkin lymphoma. *Br J Haematol* 185: 79-88, 2019.
50. Karamanos NK, Theocharis AD, Piperigkou Z, Manou D, Passi A, Skandalis SS, Vynios DH, Orian-Rousseau V, Ricard-Blum S, Schmelzer CEH, *et al*: A guide to the composition and functions of the extracellular matrix. *FEBS J* 288: 6850-6912, 2021.
51. Peltonen R, Hagström J, Tervahartiala T, Sorsa T, Haglund C and Isoniemi H: High expression of MMP-9 in primary tumors and high preoperative MPO in serum predict improved prognosis in colorectal cancer with operable liver metastases. *Oncology* 99: 144-160, 2021.
52. Wang T, Zhang Y, Bai J, Xue Y and Peng Q: MMP1 and MMP9 are potential prognostic biomarkers and targets for uveal melanoma. *BMC Cancer* 21: 1068, 2021.
53. Xu T, Gao S, Liu J, Huang Y, Chen K and Zhang X: MMP9 and IGFBP1 regulate tumor immune and drive tumor progression in clear cell renal cell carcinoma. *J Cancer* 12: 2243-2257, 2021.
54. Quintero-Fabián S, Arreola R, Becerril-Villanueva E, Torres Romero JC, Arana-Argáez V, Lara-Riegos J, Ramírez Camacho MA and Alvarez-Sánchez ME: Role of matrix metalloproteinases in angiogenesis and cancer. *Front Oncol* 9: 1370, 2019.
55. Liu C, Shen Y and Tan Q: Diagnostic and prognostic values of MMP-9 expression in ovarian cancer: A study based on bioinformatics analysis and meta-analysis. *Int J Biol Markers* 38: 15-24, 2023.
56. Jiang H and Li H: Prognostic values of tumoral MMP2 and MMP9 overexpression in breast cancer: A systematic review and meta-analysis. *BMC Cancer* 21: 149, 2021.
57. Shao W, Wang W, Xiong XG, Cao C, Yan TD, Chen G, Chen H, Yin W, Liu J, Gu Y, *et al*: Prognostic impact of MMP-2 and MMP-9 expression in pathologic stage IA non-small cell lung cancer. *J Surg Oncol* 104: 841-846, 2011.
58. Lin Z, Liu Y, Sun Y and He X: Expression of Ets-1, Ang-2 and maspin in ovarian cancer and their role in tumor angiogenesis. *J Exp Clin Cancer Res* 30: 31, 2011.
59. Zhang L, Li X, Feng X, Berkman T, Ma R, Du S, Wu S, Huang C, Amponsah A, Bekker A and Tao YX: E74-like factor 1 contributes to nerve trauma-induced nociceptive hypersensitivity through transcriptionally activating matrix metalloprotein-9 in dorsal root ganglion neurons. *Pain* 164: 119-131, 2023.
60. Wang L: ELF1-activated FOXD3-AS1 promotes the migration, invasion and EMT of osteosarcoma cells via sponging miR-296-5p to upregulate ZCCHC3. *J Bone Oncol* 26: 100335, 2020.
61. Liu Y, Ma R, Juan D, Yuan Z, Sun J, Wang M, Li Y, Bao Y and Jin H: Adipose-derived mesenchymal stem cell-loaded β -chitin nanofiber hydrogel activates the AldoA/HIF-1 α pathway to promote diabetic wound healing. *Am J Stem Cells* 12: 1-11, 2023.
62. Wang Y, Hu C, Kwok T, Bain CA, Xue X, Gasser RB, Webb GI, Boussiotas A, Shen X, Daly RJ and Song J: DEMoS: a deep learning-based ensemble approach for predicting the molecular subtypes of gastric adenocarcinomas from histopathological images. *Bioinformatics* 38: 4206-4213, 2022.
63. Bonsang B, Maksimovic L, Maille P, Martin N, Laurendeau I, Pasmant E, Bièche I, Deschamps J, Wolkenstein P and Ortonne N: VEGF and VEGFR family members are expressed by neoplastic cells of NF1-associated tumors and may play an oncogenic role in malignant peripheral nerve sheath tumor growth through an autocrine loop. *Ann Diagn Pathol* 60: 151997, 2022.
64. De Re V, Alessandrini L, Brisotto G, Caggiari L, De Zorzi M, Casarotto M, Miolo G, Puglisi F, Garattini SK, Lonardi S, *et al*: HER2-CDH1 interaction via Wnt/B-catenin is associated with patients' survival in HER2-positive metastatic gastric adenocarcinoma. *Cancers (Basel)* 14: 1266, 2022.
65. Qin X, Chen Y, Ma S, Shen L and Ju S: Immune-related gene TM4SF18 could promote the metastasis of gastric cancer cells and predict the prognosis of gastric cancer patients. *Mol Oncol* 16: 4043-4059, 2022.
66. Liu C, Omilusik K, Toma C, Kurd NS, Chang JT, Goldrath AW and Wang W: Systems-level identification of key transcription factors in immune cell specification. *PLoS Comput Biol* 18: e1010116, 2022.
67. Klugman M, Fazzari M, Xue X, Ginsberg M, Rohan TE, Halmos B, Hanna DB, Shuter J and Hosgood HD III: The associations of CD4 count, CD4/CD8 ratio, and HIV viral load with survival from non-small cell lung cancer in persons living with HIV. *AIDS Care* 34: 1014-1021, 2022.
68. Fridman WH, Petitprez F, Meylan M, Chen TWW, Sun CM, Roumenina LT and Sautès-Fridman C: B cells and cancer: To B or not to B? *J Exp Med* 218: e20200851, 2021.
69. Peña-Romero AC and Orenes-Piñero E: Dual effect of immune cells within tumour microenvironment: Pro- and anti-tumour effects and their triggers. *Cancers (Basel)* 14: 1681, 2022.
70. Dou A and Fang J: Heterogeneous myeloid cells in tumors. *Cancers (Basel)* 13: 3772, 2021.

